



Review

# A Review on the Effect of Metakaolin on the Chloride Binding of Concrete, Mortar, and Paste Specimens

Reza Homayoonmehr <sup>1</sup>, Ali Akbar Ramezanianpour <sup>2</sup>, Faramarz Moodi <sup>2,\*</sup>, Amir Mohammad Ramezanianpour <sup>3</sup> and Juan Pablo Gevaudan <sup>4</sup>

<sup>1</sup> Department of Civil Engineering, Amirkabir University of Technology, Tehran 1591634311, Iran

<sup>2</sup> Concrete Technology and Durability Research Center (CTDRc), Department of Civil & Environmental Engineering, Amirkabir University of Technology, Tehran 1591634311, Iran

<sup>3</sup> School of Civil Engineering, College of Engineering, University of Tehran, Tehran 111554563, Iran

<sup>4</sup> Department of Architectural Engineering, Pennsylvania State University, University Park, PA 16802, USA

\* Correspondence: fmoodi@aut.ac.ir

**Abstract:** Chloride binding is a complex phenomenon in which the chloride ions bind with hydrated Portland cement (PC) phases via physical and chemical mechanisms. However, the current utilization of clays as (Al)-rich supplementary cementitious materials (SCMs), such as metakaolin (MK), can affect the chloride-binding capacity of these concrete materials. This state-of-the-art review discusses the effect of clay-based SCMs on physical and chemical chloride binding with an emphasis on MK as a high-reactivity clay-based SCM. Furthermore, the potential mechanisms playing a role in physical and chemical binding and the MK effect on the hydrated cement products before and after exposure to chloride ions are discussed. Recent findings have portrayed competing properties of how MK limits the physical chloride-binding capacity of MK-supplemented concrete. The use of MK has been found to increase the calcium silicate hydrates (CSH) content and its aluminum to silicon (Al/Si) ratio, but to reduce the calcium to silicon (Ca/Si) ratio, which reduces the physical chloride-binding capacity of PC-clay blended cements, such as limestone calcined clay cements (LC3). By contrast, the influence of MK on the chemical chloride capacity is significant since it increases the formation of Friedel's salt due to an increased concentration of Al during the hydration of Portland cement grains. Recent research has found an optimum aluminum to calcium (Al/Ca) ratio range, of approximately 3 to 7, for maximizing the chemical binding of chlorides. This literature review highlights the optimal Al content for maximizing chloride binding, which reveals a theoretical limit for calcined clay addition to supplementary cementitious materials and LC3 formulations. Results show that 5–25% of replacements increase bound chloride; however, with a higher percentage of replacements, fresh and hardened state properties play a more pivotal role. Lastly, the practical application of four binding isotherms is discussed with the Freundlich isotherm found to be the most accurate in predicting the correlation between free and bound chlorides. This review discusses the effects of important cement chemistry parameters, such as cation type, sulfate presence, carbonation, chloride concentration, temperature, and applied electrical fields on the chloride binding of MK-containing concretes—important for the durable formulation of LC3.

**Keywords:** metakaolin; low-CO<sub>2</sub> concrete; sustainable construction; chloride binding; chloride-induced corrosion; chloride-binding isotherms



**Citation:** Homayoonmehr, R.; Ramezanianpour, A.A.; Moodi, F.; Ramezanianpour, A.M.; Gevaudan, J.P. A Review on the Effect of Metakaolin on the Chloride Binding of Concrete, Mortar, and Paste Specimens. *Sustainability* **2022**, *14*, 15022. <https://doi.org/10.3390/su142215022>

Academic Editor: Byungik Chang

Received: 14 October 2022

Accepted: 9 November 2022

Published: 14 November 2022

**Publisher's Note:** MDPI stays neutral with regard to jurisdictional claims in published maps and institutional affiliations.



**Copyright:** © 2022 by the authors. Licensee MDPI, Basel, Switzerland. This article is an open access article distributed under the terms and conditions of the Creative Commons Attribution (CC BY) license (<https://creativecommons.org/licenses/by/4.0/>).

## 1. Introduction

The use of calcined clays has attracted global research attention as a widely accessible supplementary cementitious material (SCM) with a significant chance of reducing the carbon-intensive emissions associated with the production of Portland cement [1]. Considering the limitation of industrial byproducts, such as silica fume (SF), ground granulated blast-furnace slag (GGBS), and fly ash (FA), the global availability of clays, as well as the

accessibility to calcination technology, have been poised as major contributors to the use of clays as SCMs and key components in the formulation of limestone calcined clay cement (LC3) to reduce Portland cement consumption and consequently reduce the Carbon dioxide ( $\text{CO}_2$ ) emission of the cement industry [2–7]. The environmental advantage of SCMs, particularly MK, is mainly ascribed to less required production of energy raw material and less  $\text{CO}_2$  emission in the production process and indirectly by increasing the elongating cement service life [4]. The calcination of kaolin clays, which contains 40–45 wt.%  $\text{Al}_2\text{O}_3$  [4,8,9], improves their reactivity and renders them metakaolin (MK). The reactivity improvements are due to the dehydroxylation and destruction of the plate-like morphology of the kaolin clay [1,10]. When compared to other SCMs, such as SF, GGBS, or FA, MK contains the highest alumina content [11]. As a result, these calcined clays can be utilized to replace Portland cement and reduce the clinker-to-cement ratio [12–15]. Note that MK has a great potential to be consumed solely or in combination with other SCMs in different types of concrete, such as fiber-reinforced concrete, self-compacting concrete, pervious concrete, and shotcrete [4].

In addition to improvements in the embodied carbon of concrete materials with clay-based SCMs, recent research has demonstrated the refinement of the pore structure resulting in improved mechanical and durability properties [4]. These effects are attributed to the pozzolanic reaction of the silica and alumina content with calcium hydroxide (CH) to produce additional calcium silicate hydrates (CSH), calcium aluminosilicate hydrates (CASH), and calcium aluminate hydrates (CAH). The formation of binder phases enables the porosity to decrease with a concomitant reduction in non-load bearing phases, such as CH. Other potential mechanisms such as physical filling also play a role [4,10,16]. However, replacing Portland cement with clay-based SCMs also has an important effect on lowering the alkalinity of the pore solution, which has implications for the durability of the concrete material—especially for global durability challenges such as the corrosion of reinforced concrete structures.

The corrosion of embedded reinforcement in reinforced concrete structures is one of the most pervasive global durability challenges [17–21]. The utilization of clay-based SCMs can compromise the durability of concrete materials due to the reduced alkalinity of the pore solution chemistry which is an important factor in arresting chloride-induced electrochemical corrosion of embedded reinforcement [22,23]. Reductions in the pore solution alkalinity can lead to the pH-dependent breakdown of the passive layer by reversing the chemical hydroxylation of the iron metal surface during passivation; for which, see work by [24]. It is well established that the presence of chlorides accelerates the dissolution of iron metals via the formation of iron complexes. Recent research has shown that while Fe (II)/Fe (III) chloride complexes may negligibly increase the solubility of iron, the temporary formation of nano-sized particles of chloride green rust, GR ( $\text{Cl}^-$ ), as stabilized by Ph and  $\text{O}_2$  conditions, can mediate the transport and precipitation of iron rust products far from the steel-concrete interface [25]. These recent findings add complexity to the simplified understanding of electrochemical corrosion which has often relied on simplified critical chloride thresholds ( $C_{\text{crit}}$ ) to indicate the start of the passive layer breakdown and subsequent deleterious corrosion [21,26–28]. Thus, further work is needed to understand the stabilization of GR ( $\text{Cl}^-$ ) products in relation to the steel–concrete interface characteristics [29]. These results will then need to be benchmarked by the chloride ion immobilization potential due to the phase assemblages of the cementitious material.

The utilization of calcined clays as SCMs may counteract these durability limitations via the formation of layered double hydroxide (LDH) phases that can arrest the transportation of deleterious anions, such as  $\text{Cl}^-$  and  $\text{CO}_3^{2-}$ —major culprits in the chloride-induced electrochemical corrosion of reinforced concrete structures [30]. The alumina chemical reactivity of clays is critical for the formation of chloride-binding phases [31]. For example, all alumina in GGBS is amorphous with high activity [32]; however, 20–25% of alumina in fly ash is crystalline and, hence, exhibits less chloride-binding potential than the alumina content of GGBS [31]. Chloride binding is generally considered to be a physical

or chemical process [33–35]. The chemical binding of chlorides has been attributed to Friedel’s salt ( $\text{Ca}_3\text{Al}_2\text{O}_6 \cdot \text{CaCl}_2 \cdot 10\text{H}_2\text{O}$ ) formation [36], while physical chloride binding occurs when the chloride ions are physically adsorbed on the surface of the hydration products. Such chloride binding results in reduced chloride diffusion. Badogiannis et al. [37] and Wang et al. [38] investigated the effect of chloride binding on apparent chloride diffusion and found that chloride binding significantly reduces the apparent chloride diffusion and consequently increases the time to corrosion initiation. This increase in chloride binding leads to a higher concentration of surface chloride ( $C_s$ ) exposed to marine environments [39]. However, a complete understanding of chloride binding when utilizing clays requires an in-depth discussion of the recent progress in characterizing and evaluating the cement chemistry factors controlling the immobilization of chlorides.

This state-of-the-art review discusses recent mechanistic findings on the effect of using calcined clays, such as MK, on the chloride-binding capacity of concrete materials, such as LC3 formulations. In this review, we present recent advances in our understanding of both the physical and chemical chloride-binding mechanisms as influenced by clay SCMs. In order to fully understand these mechanisms, the influential parameters for chloride binding, such as the sulfate presence, carbonation, temperature, chloride concentration, cation type, applied electrical field, and binding isotherms, are further explained.

## 2. Physical Chloride Binding of Specimens Containing MK

Physical binding is generally attributed to the attachment and accumulation of chloride ions on the surface of hydrates. Three potential mechanisms have been proposed by Ramachandran: a chemisorbed layer on the CSH surface, bound Cl between CSH layers, and bound Cl in the CSH lattice [40,41]. Most of the physically bound chlorides are generally attributed to chloride ions bound in the ion-exchange sites of CSH and CASH. This bound mechanism differs as the composition of CSH and CASH is affected by the calcium to silicon (Ca/Si) ratio or calcium ion concentration in concrete formulations [31,42–45]. Most of the physically adsorbed chloride is adsorbed by CASH gel; the chloride adsorption by CH, ettringite, and Friedel’s salt is neglected because of their small surface area compared to CSH or CASH binder gels [46,47].

As previously mentioned, one of the parameters that significantly affects the physical binding capacity of Portland cement materials is the Ca/Si ratio of CSH [31,48]. More specifically, a reduction in the Ca/Si ratio reduces the physical capacity of the chloride binding of CSH [31,41,49]. The average Ca/Si ratio in CSH is around 1.75 with a general range of 0.7 to 2.0 [48]. Gue et al. [31] indicated that replacing Portland cement with 4% MK does not significantly change the Ca/Si ratio; however, the replacement level of 16% slightly decreases the Ca/Si ratio. Shi et al. [50] also observed a reduction in the Ca/Si ratio in the mortar specimens containing 31.9% of MK and specimens containing 25.5% of MK and 6.4% of limestone compared to the control specimens made with white Portland cement. This binding reduction effect can be explained by the increase in the chain length of CSH [51] which leads to the transformation of the CSH structure from amorphous to layered with fewer binding sites and more distance between CSH layers [52], decreasing calcium availability and leading to a net positive charge on the CSH surface, as well as increasing the deprotonated silanol group on the CSH surface [53]. In this regard, Zhao and Khoshnazar [54] reported that the Ca/Si ratio did not significantly decrease in specimens containing 40% MK compared to 20% MK. This is in accordance with the results reported for LC3 containing 50% and 95% of MK [55,56]. On the other hand, further research is needed to understand how MK may also help increase the physical chloride binding due to an increase of poorly chloride-binding CSH and CASH binder phases [33,57].

In contrast, using conventional replacement levels of MK (5–25%) increases the aluminum to silica (Al/Si) ratio of CSH, and thereby the aluminosilicate chain length [54,58,59]. Increasing the Al/Si ratio of CSH enhances binding capacity by substituting  $\text{Al}^{3+}$  for  $\text{Si}^{4+}$ , leading to more potential binding sites [31,47,60]. This effect may help to compensate for the negative effect of MK on the physical binding capacity by decreasing the specific surface

area of CSH [31]. However, physically bound chloride is usually a small proportion of the total bound chloride, and the majority of chloride binding occurs in the form of chemical chloride binding [61,62].

### 3. Chemical Chloride Binding of Specimens Containing MK

Chemical binding is generally attributed to Friedel's salt formation, mainly from the Tricalcium Aluminate ( $C_3A$ ) phase of Portland cement and reactive alumina of SCMs (see Table 1) [31,46,61,63,64]. The use of clays, such as MK, increases alumina, ferric oxide, and monosulfate (AFm) phases due to the high amount of aluminum ions during early cement hydration reactions. AFm phases can contribute to chemical chloride binding via the conversion to Friedel's salt through a chloride anion exchange [31,46,64–67]. In this regard, Gue et al. [31] showed a linear relation between chemically bound chloride and Friedel's salt intensity in SF and MK-containing pastes (see Figure 1). There are two main formation mechanisms of Friedel's salt, namely adsorption and anion exchange. In adsorption and anion exchange,  $Na^{2+}$  and  $OH^-$  are released, respectively [44,68]; thus, chloride binding affects the chemistry of pore solution and increases its pH [44,67–69].

**Table 1.** Chloride content in pastes calculated using the equilibrium method (g per 100 g paste). Adapted with permission from Ref. [64].

Replacement Level	Portland Cement–Metakaolin Pastes			Reference Pastes		
	10%	20%	30%	10%	20%	30%
Total chloride	1.29	1.11	0.61	1.03	0.90	0.66
Free chloride	0.15	0.11	0.10	0.27	0.26	0.27
Bound chloride	1.15	1.00	0.51	0.76	0.63	0.38
Chloride calculated by Friedel's salt content	1.30	0.93	0.08	0.50	0.35	0.23

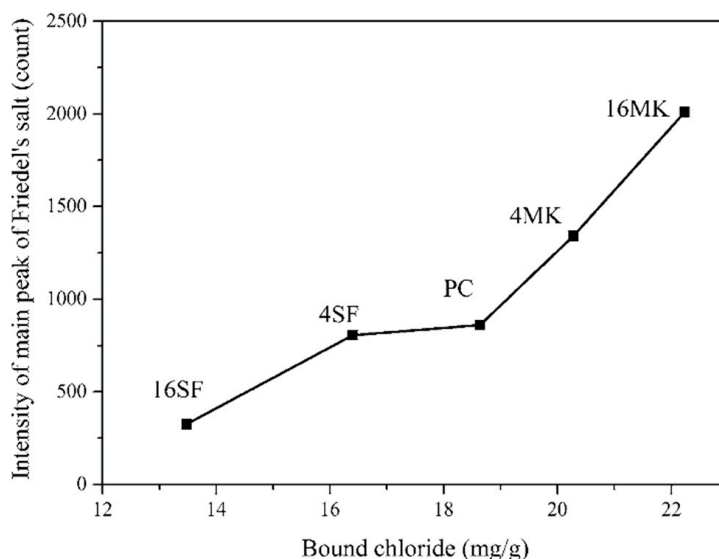


**Figure 1.** The relationship between the diffraction peak intensity of Friedel's salt and total bound chloride in cement pastes. Adapted with permission from Ref. [31].

Generally, the amount of chemical binding chloride depends mostly on phase assemblage rather than just aluminum availability [38,64]. Wang et al. [38] reported an optimum range for  $Ca/Al$  in which the chloride binding is maximized. Figure 2 shows the optimum range for the  $Ca/Al$  ratio, which ranges from 3 to 7. In higher ratios calcium and in lower ratios aluminum is excessive. The optimum  $Ca/Al$  ratio depends on parameters such as the sulfate content in cement, the alumina and calcium in the inert component in the mineral admixture, and the hydration degree of cementitious materials. They observed increasing

chloride-binding capacity with partial replacement of cement with MK and FA in the presence of 7% limestone. However, in cases of high replacement levels of Portland cement with Al-rich SCMs, such as MK, the chloride-binding capacity decreased because of insufficient calcium ions for further reaction as these are utilized in the pozzolanic reaction and to some extent by C<sub>3</sub>A dilution. They observed that specimens containing 10% MK and a blend of 5% and 20% of MK and FA, respectively, had the most chloride binding. By increasing MK and FA to 10% and 20%, respectively, the chloride-binding capacity decreased, but it still had more bound chloride than the control specimen [38]. These findings regarding the optimum range of Ca/Al for increasing the chloride-binding potential can be beneficial for designing LC3 formulations with superior durability against chloride-induced corrosion of steel reinforcement [38]. However, more research is needed to ascertain optimal clay supplementation proportions. For example, Gbozee et al. [64] indicated that pastes with 10% MK are more capable of chemical chloride binding than pastes with 20% and 30%, which is attributed to the decrease in sulfate and calcium ions due to the dilution effect and pozzolanic reaction. However, Dousti et al. [41] observed that specimens containing 33.33% MK had greater chloride-binding capacity than the specimens with 50% and 66.66% MK. These chloride-binding capacity results related to OPC-MK-lime paste formulations where an increased Ca/Al ratio decreased the chemical chloride-binding potential significantly.

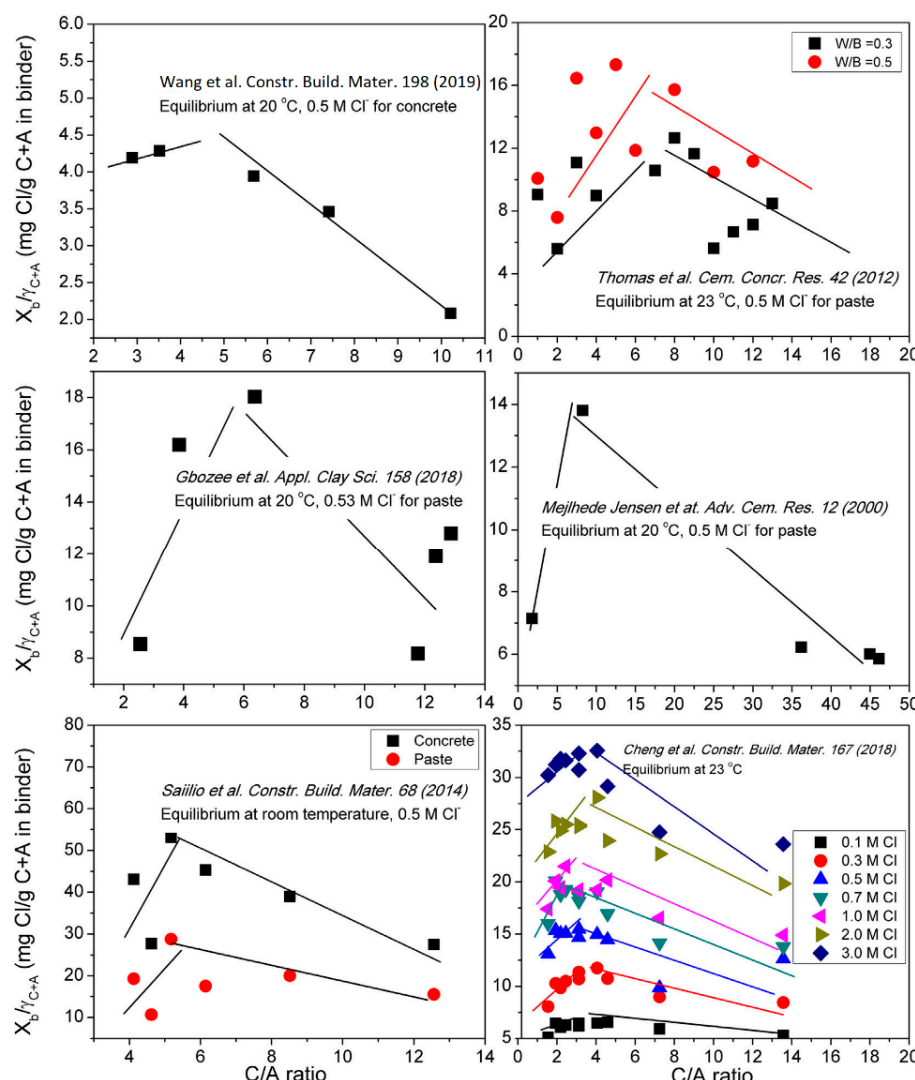


**Figure 2.** Relationship between chloride-binding capacity and CaO to Al<sub>2</sub>O<sub>3</sub> (C/A) ratio of binder. Adapted with permission from Ref. [38].

As mentioned previously, the majority of the total bound chloride is comprised of chemical bound chloride, especially for exposures to conventional chloride concentration. It was seen that in MK-lime pastes with a MK: lime ratio of 1:1, 60–65% of the total chloride was bounded chemically [68]. This is in line with research on the chloride binding of LC3s which contain 20–30% clay replacements [50,53]. However, a reliable method for measuring the amount of chemically bound chloride and its proportion to total bound chloride has not been proposed because of its complexity, especially in blended cements [50]. Figure 3 shows that MK positively affects chemically bound chloride but does not significantly increase the physically bound chloride due to the aforementioned competing factors [50]. Gue et al. [31] concluded that unlike SF, which reduces the total bound chloride, using 16% MK increases the total bound chloride mainly by increasing the chemically bound chloride—a two-fold increase in the chemically bound chloride when compared to non-supplemented Portland cement.

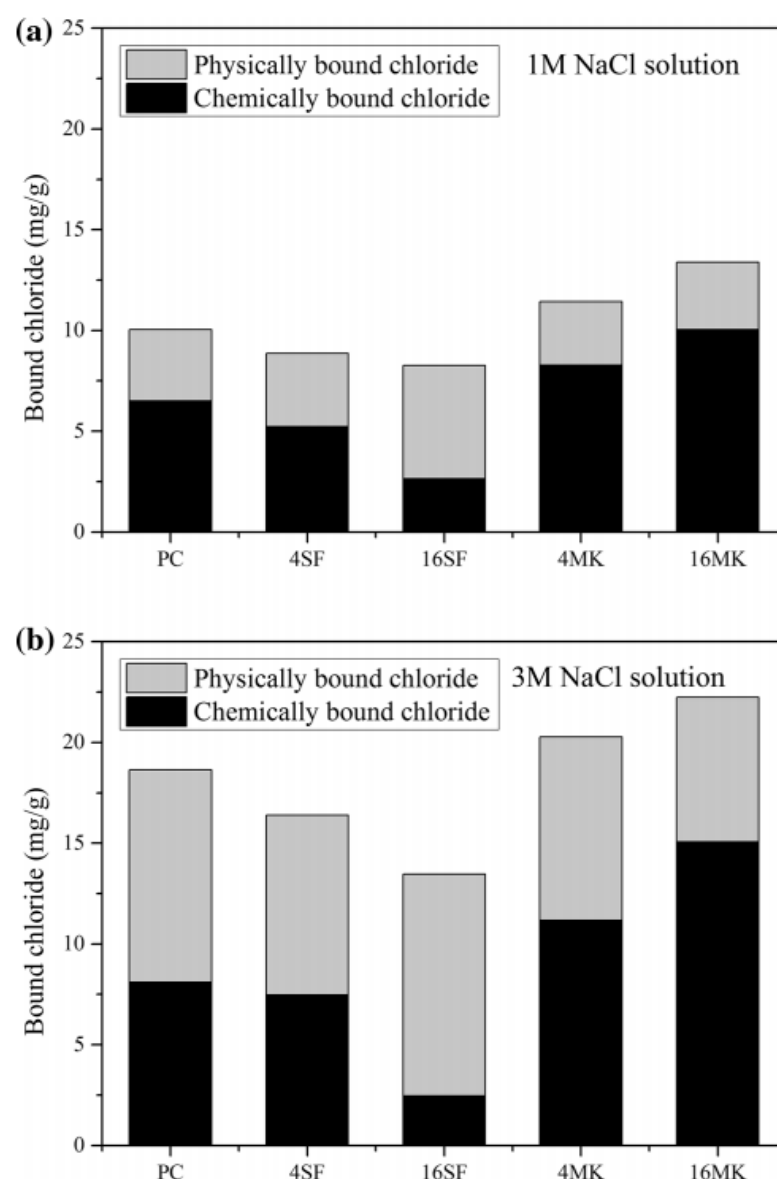


**Figure 3.** The amounts of physically and chemically bound chlorides in cement pastes after equilibrium binding in NaCl solutions. (a) 1 mol/L NaCl solution; (b) 3 mol/L NaCl solution (PC: Portland cement paste; 4SF: paste containing 4% of SF; 16SF: paste containing 16% of SF; 4MK: paste containing 4% of MK; 16MK: paste containing 16% of MK). Adapted with permission from Ref. [31].

### The Effect of MK on Hydrated Cement Products before and after Exposure to NaCl

Prior to exposure to NaCl solutions, ettringite, AFm phases, and strätlingite are usually observed in Portland cement–MK blends [31,50,70,71]. The amount of ettringite and calcite in specimens containing MK has been proved to be less than OPC, as shown in SEM images and X-ray diffraction (XRD) [31,50,64,72]. Moreover, the formation of monocarboaluminate has been reported to remain unchanged [64] or increase [31] in OPC-MK materials, when compared with non-supplemented OPC materials.

Following exposure of MK containing pastes to a NaCl solution, the amount of monosulfoaluminate decreases to form Friedel's salt. In fact, each gram of monosulfoaluminate forms around 0.9 g of Friedel's salt [64]. More specifically, the chloride ions take the place of sulfate ions in monosulfoaluminate to form Kuzel's salt and, consequently, Friedel's salt [68]. However, the released sulfate ions can cause delayed ettringite formation, which can be a reason for the degradation of structures in the marine environment [38,51,68,73–75] and may also lead to further monosulfoaluminate formation in the presence of MK [64].

In comparison with monosulfoaluminate, monocarboaluminate contributes less to the chemical binding of chloride ions. Monocarboaluminate contributes to the chemical binding of chloride ions by exchanging  $\text{CO}_3^{2-}$  with chloride ions; then the released  $\text{CO}_3^{2-}$  is bound in calcite [41,64,71,75,76]. Therefore, the contribution of monocarboaluminate to chloride binding and Friedel's salt formation depends on calcium availability [50,71,77], and no or very low calcium carbonate precipitation is predicted [50]. It is noteworthy that, due to pozzolanic reaction and consequent reduction of  $\text{CaOH}_2$  and calcium availability, the contribution of monocarboaluminate to chloride binding in MK-containing pastes decreases [64]; therefore, monocarboaluminate is understood to be more thermodynamically stable than monosulfoaluminate [76]. The mentioned effect of calcium on chloride binding has also been confirmed in other studies [38,69,78].

Strätlingite does not change significantly with exposure to NaCl [64,68], but Zibara et al. [71] concluded that in high chloride concentrations, Strätlingite converts to Friedel's salt at a slow rate, and this conversion is mostly limited by calcium availability [50]. Dousti et al. [41] also indicated that Strätlingite decreases in higher chloride concentrations, which was observed better in specimens with a MK: lime ratio of 1:2 than in the ones with a 2:1 ratio. When exposed to NaCl solution, the amount of ettringite increases [64,75], which shows that it does not contribute to chloride binding [64,79]. However, it may slightly reduce the chloride-binding capacity by reducing monosulfoaluminate availability due to delayed ettringite formation [64], as previously discussed.

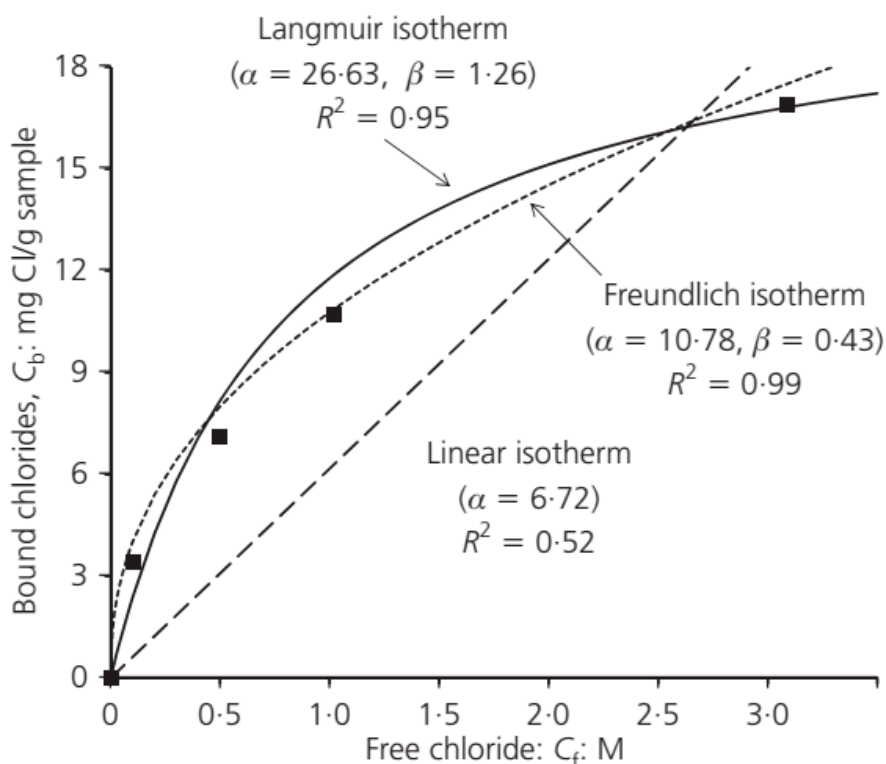
#### 4. Binding Isotherms

As previously laid out, the measurement of chlorides using cementitious materials is a complex mechanism. A common method to test the chloride binding of cementitious materials is by determining their binding isotherms which describe the relationship between free and binding chlorides. To investigate their accuracy, other parameters like temperature and  $\text{OH}^-$  leakage should be taken into consideration. Four main types of binding isotherms have been proposed, namely, linear, Langmuir, Freundlich, and Brunauer, Emmett, and Teller (BET) binding isotherm [44]; however, none of these can accurately and comprehensively capture the binding of chloride anions by multi-phasic materials, such as OPC materials (See Table 2).

**Table 2.** Isotherm relations ( $k$ ,  $\alpha$ , and  $\beta$  are binding constants).

Isotherm	Relation
Linear binding isotherm	$C_b = kC_f$
Langmuir isotherm	$C_b = \frac{\alpha C_f}{(1+\beta C_f)}$
Freundlich binding isotherm	$C_b = \alpha C_f^\beta$
Brunauer, Emmett, Teller (BET) isotherm	$\frac{C_b}{C_{bm}} = \frac{\alpha \frac{C}{C_S} [1 - (1-\beta)(1-\beta \frac{C}{C_S})^2]}{\beta(1-\beta \frac{C}{C_S})(1-\beta \frac{C}{C_S} + \alpha \frac{C}{C_S}(1-\beta \frac{C}{C_S} + \frac{C}{C_S}))}$

In general, recent findings have confirmed the acceptable accuracy of Langmuir and Freundlich isotherms to represent the chloride binding of OPC-MK materials [38,80–83]. The linear isotherm is oversimplified to indicate the relation between free and bind chloride in real cases [38,44,84] and has more accuracy in chloride concentrations below 20 kg/m<sup>3</sup> and over long-term periods (10–30 years) [84]. The Langmuir isotherm has an acceptable accuracy in low chloride concentrations, and the BET isotherm is rarely used due to its complexity. The Freundlich isotherm seems the most approximate in normal seawater [44]. It has been reported that choosing a binding isotherm critically affects service life prediction [85]. As can be observed in Figure 4, Dousti and Shekarchi [86] described the non-linear behavior of both the Langmuir and Freundlich isotherms as matching experimental data on experimental bound and free chloride concentrations with a coefficient of discrimination ( $R^2$ ) of 0.95 and 0.99, respectively. These results were extrapolated for other concrete materials of varying formulations and it was found that the Freundlich isotherm provides a better fit than other isotherms (see Figure 5). Importantly for these results, the variables of the Freundlich isotherm ( $\alpha$  and  $\beta$ ) were demonstrated to be a function of temperature as well as cementing material type. Note that  $\alpha$  and  $\beta$  have no physical meaning and also depend on the units of  $C_b$  and  $C_f$  [44].

**Figure 4.** Idealized binding isotherms for OPC paste with W/C = 0.4 and an exposure temperature of 22 °C. Adapted with permission from Ref. [86].

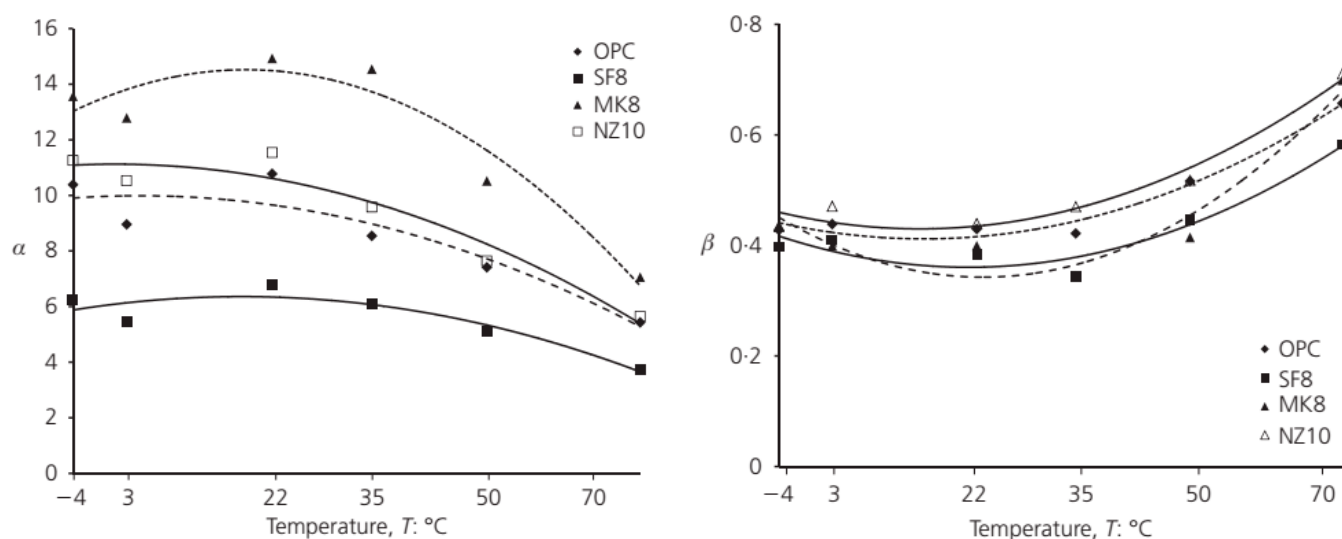


**Figure 5.** Coefficients in a Freundlich binding isotherm at exposure temperature  $T$ : (left)  $\alpha$ , (right)  $\beta$ . Adapted with permission from Ref. [86].

## 5. Other Effective Parameters for Chloride Binding

### 5.1. Effect of Hydrotalcite

While not present in MK-OPC materials, hydrotalcite is an important LDH phase that forms with Mg-containing precursors, such as GGBS [87,88]. The presence of LDHs, such as hydrotalcite, increases the chloride binding of the cementitious materials in general. Machner et al. [89] studied the effect of hydrotalcite on the chloride-binding capacity of pastes containing Portland cement, limestone, MK, and Mg-containing dolomite. They observed that specimens containing MK with limestone or dolomite have greater chloride-binding capacity, which can be partly ascribed to the hydrotalcite formation in the dolomite reaction and its positive effect on chloride binding. According to this study and previous studies [90–92], Al-rich SCMs like MK decrease the magnesium to alumina ( $Mg/Al$ ) ratio of hydrotalcite, which decreases its chloride-binding capacity. However, this finding is in contradiction to a previous study [93].

### 5.2. Effect of Gypsum and Sulfate Ion

The gypsum that is present in Portland cement may affect chloride binding as it does on MK hydration products. Sufficient gypsum (more than 8%) favors the ettringite production from the reaction of sulfate with  $C_3A$  and inhibits strätlingite and  $C_4AH_{13}$  formation [94,95]. Moreover, investigating the effect of gypsum on chloride-binding capacity is important in designing Al-rich SCMs according to increased chloride resistance [68]. It has been shown that using 4% of gypsum in MK-lime paste supports the formation of monosulfoaluminate and reduces strätlingite and monocarboaluminate peaks; at 8% of gypsum, the amount of ettringite significantly increases, and monosulfoaluminate seems to be restrained, which means that monosulfoaluminate can transform to ettringite by adding gypsum [68]. As shown in Figure 6, Wand et al. [68] indicated that by using 4% and 8% of gypsum in MK-lime pastes, chloride binding was reduced by 9% and 10.5%, respectively, after equilibrium time (3 h) [68]. This reduction is attributed to the competition between  $SO_4^{2-}$  and  $Cl^-$  to form AFm phases and to physically be adsorbed by the CSH phase beside the dilution of MK [44,53,96,97]. The negative effect of gypsum on the chloride-binding capability has been shown in other studies [96,98].

### 5.3. Effect of Carbonation

Carbonation has also been suggested to reduce binding-chloride capacity [44,99,100]. This is because carbonation reduces pH and consequently increases Friedel's salt solubility [44,67,77,101,102]. Carbonation also increases the negative potential of CSH, leading to less adsorbed chlorides [103].

Furthermore, due to the increase of the carbonate content, chloride and carbonate compete to form AFm phases [100]. Therefore, it has been concluded that chemical chloride binding is reversible if carbonation happens [44,104]. By progressing carbonation and lowering pH less than a certain amount of about 10.5 to 10.7, and removing  $\text{Ca}^{2+}$ , the solubility of ettringite increases and may decompose to gypsum and aluminate sulfate [67,105,106], but the stratingite still remains stable [68]. Figure 7 illustrates the effect of the carbonation progress on the pH and chloride binding of MK-lime paste specimens with 0%, 4%, and 8% of MK. However, carbonation may also have a beneficial effect on chloride binding by consuming hydroxyl and, as a result, reducing the competition between hydroxyls and chlorides [68]. This presents a critical gap in knowledge as it relates to the long-term carbonation effects on the chloride binding of OPC-clay blended materials and LC3s.

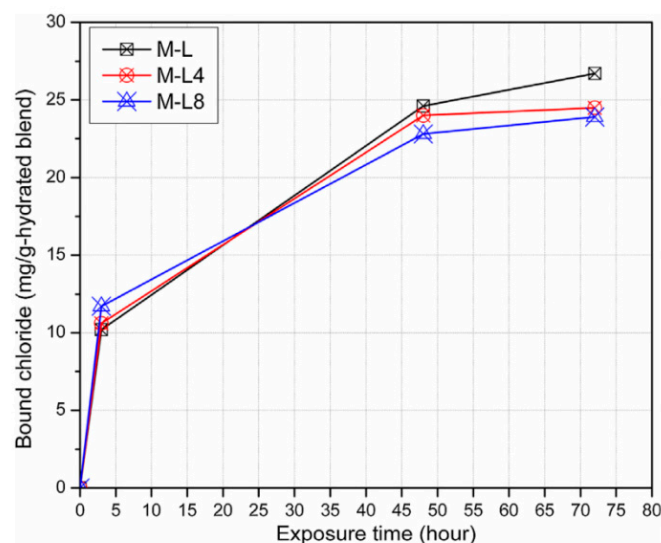


**Figure 6.** Chloride-binding content during exposure (MK-Lime (M-L) paste and 0%, 4%, 8% gypsum). Adapted with permission from Ref. [68].

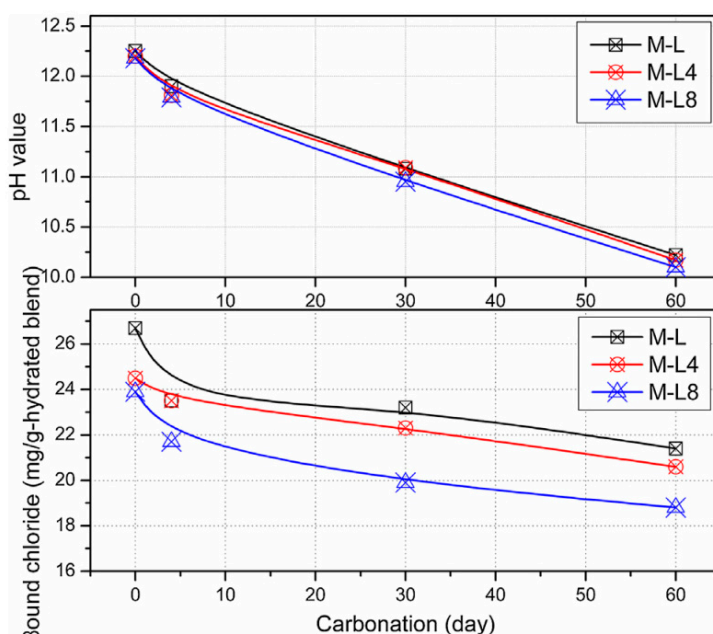


**Figure 7.** Bound chloride and PH value of exposure solution during carbonation (MK-lime (M-L) paste and 0, 4, 8% gypsum). Adapted with permission from Ref. [68].

#### 5.4. Chloride Concentration

The higher chloride concentration of external and pore solutions increases chloride binding and then reaches a plateau [31,38,41,44,50,89]. Machner et al. [89] demonstrated that OPC pastes containing MK and carbonate (dolomite and limestone) reach a plateau in higher chloride concentration. Gue et al. [31] concluded that external chloride concentration influences the physical chloride binding more significantly. Dousti et al. [41] indicated that the amount of bound chloride increases at a steep slope in exposure to 0.1–1.0 M of chloride concentration; then, at higher chloride concentrations, chloride binding increases just at a slow slope.

#### 5.5. Compound Composition of Portland Cement

The Al-composition of Portland cement ( $C_3A$  and Tetracalcium Aluminoferrite ( $C_4AF$ )) plays the most critical role in the chemical binding of chlorides between clinker compounds, particularly  $C_3A$  compounds that have three times more binding capacity and a greater reaction rate than  $C_4AF$  [44,107] and its reaction rate [37]. Furthermore, it has been shown that the amount of CSH influences chloride binding, especially physical binding [81]; therefore, Tricalcium Silicate ( $C_3S$ ) and Dicalcium Silicate ( $C_2S$ ) in cement also affect the binding capacity indirectly by forming CSH, but on a smaller scale than  $C_3A$  and  $C_4AF$  [44].

#### 5.6. Hydroxyl Ion ( $OH^-$ ) Concentration and pH

A lower pH increases the bound-chloride capacity [69,108,109] due to less competition between hydroxyl and chloride ions to be adsorbed in the surface of layers and also decreasing solubility of Friedel's salt [44,50,53]. The reduction of pH also leads to the limited dissolution of portlandite [69,89]. It is worth noting that a lower pH is expected for pastes containing different SCMs such as MK and MK-lime pastes and ones exposed to higher salt-solution concentrations [89,110,111].

The pH of the external solution also influences the chloride-binding capacity as well as the concentration of the  $OH^-$  ions in the pore solution. According to De Weerd et al. [109], regardless of the type of salt, there is a linear relation between the pH of the external solution and chloride-binding capacity. Shi et al. [112] observed that the pH of the exposure solution could also govern the effect of different cations on the binding of chloride (see Figure 8) [50]. However, a significant reduction of pH is observed in Portland cement, MK, and MK-lime pastes exposed to  $CaCl_2$  [50,69,89,113], which may be caused by calcium binding with CSH and release of  $H^+$  (see Figure 9) [50,89]. This reduction leads to increased chloride binding, which in OPC is generally physical, and in MK and MK-lime containing pastes is primarily chemical [50]. Furthermore, exposure to  $NaCl$  and subsequent  $OH^-$  release due to the formation of Friedel's salt, calcium carbonate, and sodium hydroxide has a slight incremental effect on pH, which has a minor effect on chloride binding [50].

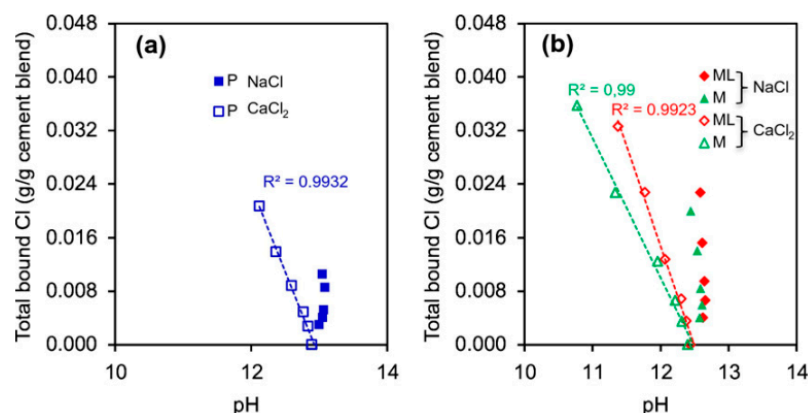


**Figure 8.** Relationship between the total bound chloride and the pH of the exposure solutions for (a) Portland cement (P) paste and (b) the metakaolin-limestone (ML) and metakaolin (M) pastes exposed to the  $NaCl$  and  $CaCl_2$  solutions. Adapted with permission from Ref. [50].

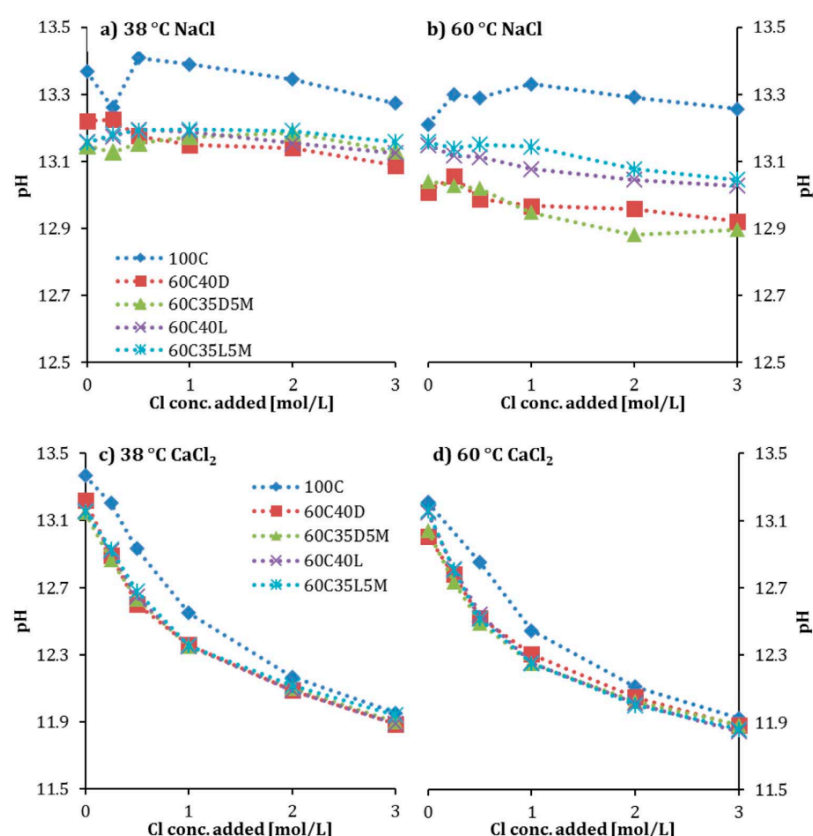


**Figure 9.** pH measurements of the supernatant of the various binder compositions cured at 38 °C or 60 °C and exposed to various concentrations of NaCl or CaCl<sub>2</sub>. The measurements were performed at 20 °C. The points at 0 mol/L refer to the pH measurements of the reference samples exposed to deionized water. Adapted with permission from Ref. [89].

##### 5.7. Cation

The cation of chloride salt (e.g., Ca<sup>2+</sup>, Mg<sup>2+</sup>) has been shown to make a noticeable difference in chloride binding [57]. Neat OPC paste, MK-supplemented materials, and LC3 materials exposed to CaCl<sub>2</sub> and MgCl<sub>2</sub> were found to have more bound chloride ions than when exposed to the same concentration of chloride in NaCl solutions (see Figure 10) [42,57,69,108,109,114]. This elucidates a potential cation type effect on the chloride adsorption where an increasing positive charge of the surface of C(A)SH and a higher calcium concentration [44,50,57,89] as well as an increase in AFm formed is apparent [57]. Moreover, Machner et al. [89] also observed five to ten times higher chloride binding and more bound chlorides to C(A)SH in specimens exposed to CaCl<sub>2</sub> than to NaCl. Babaahmadi et al. [57] reported around two times more bound chloride in paste specimens containing 15% of MK in exposure to CaCl<sub>2</sub> compared to NaCl. Shi et al. [50] reported that in exposure to CaCl<sub>2</sub>, there is a linear correlation between the bound calcium content (uptake of calcium by hydration products) and bound chloride content with a Cl:Ca ratio of approximately 2:1 for tested cement blends (see Figure 11) [50]. They also reported calcium carbonation precipitation due to Friedel's salt formation from the transformation of monocarboaluminate.

##### 5.8. Temperature

In most studies, high temperature has been shown to increase the rate of chloride ingress in concrete [41,115,116] and to reduce the chloride-binding capacity [44]. For instance, the chloride corrosion rate in the Persian Gulf is about eight times higher than in the Nordic area due to the higher average temperature [117]. High temperature increases the ionic vibration of chloride ions which leads to the higher likelihood of release from

physical absorption [116,118]. Alternatively, in the case of chemically bound chloride, high temperature can have both positive and negative effects. High temperatures can reduce bound chlorides by increasing the solubility of binding products, such as Friedel's salt. In contrast, the chemical binding rate may also be accelerated due to temperature increases [41,44,118]. Hence, this remains an important parameter to control in experimental programs of chloride binding. Zibara [113] concluded that at low chloride concentrations (0.1–1.0 M), the higher temperature reduces the bound chloride and increases the bound chloride in high concentrations (3 M). Dousti and Shekarchi [86] and Dousti et al. [41] showed that in OPC specimens and pastes containing MK, SF, and NZ in a range of 0.1 to 3.0 M of NaCl solution, chloride binding decreased by increasing temperature, except for 22 °C, which had the greatest chloride binding (see Figures 12 and 13). This result was in accordance with the XRD result and Friedel's salt amount. Machner et al. [89] also reported that chloride binding in Portland cement specimens containing limestone and MK is lower in curing temperature of 60 °C than 38 °C [89]. Table 3 also indicates the effect of increasing temperature on chloride-binding content from some older research.

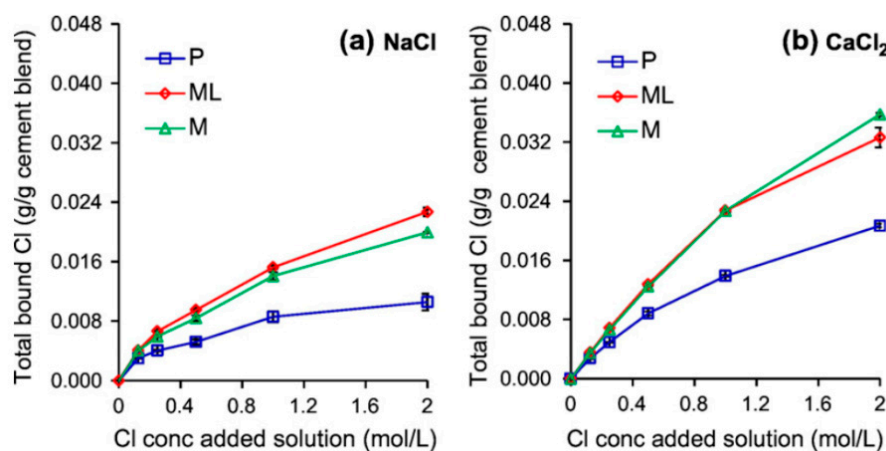


**Figure 10.** Chloride-binding isotherms for Portland cement (P), metakaolin-limestone (ML) and metakaolin (M) pastes exposed to (a) NaCl and (b) CaCl<sub>2</sub> solutions. The bound chloride content is reported as g per g of unhydrated cement blend and shown as a function of the concentration of added chloride ions in the exposure solutions. Adapted with permission from Ref. [50].

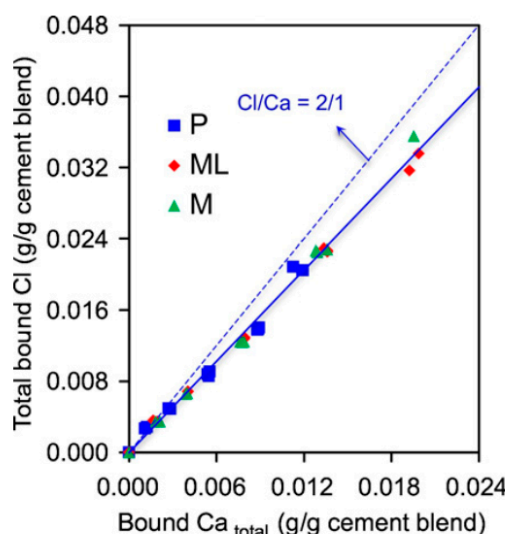


**Figure 11.** Relationship between the total bound chloride and the total "bound" calcium (i.e., uptake of calcium from the CaCl<sub>2</sub> exposure solution by hydration products) for pastes exposed to the CaCl<sub>2</sub> solution. Adapted with permission from Ref. [50].

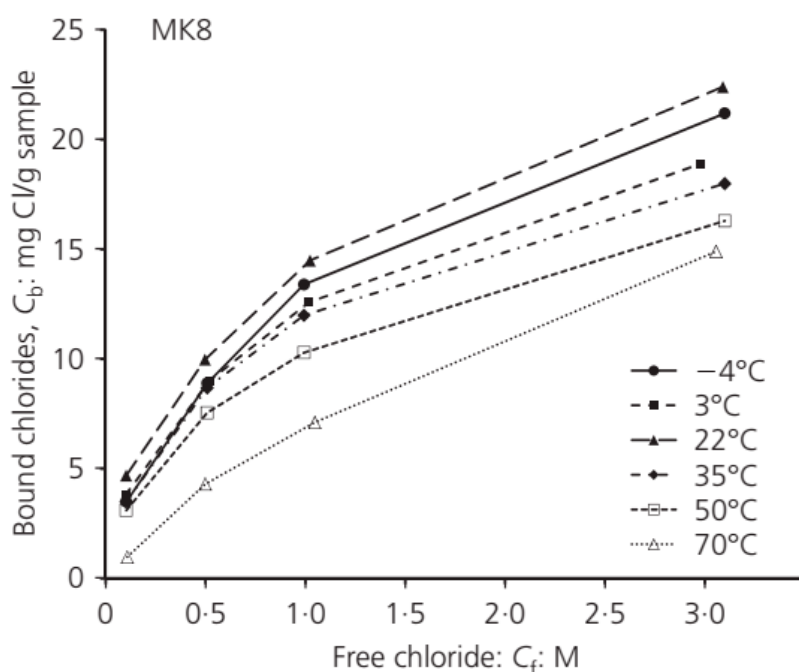


**Figure 12.** Chloride-binding isotherm for paste containing 8% MK. Adapted with permission from Ref. [86].

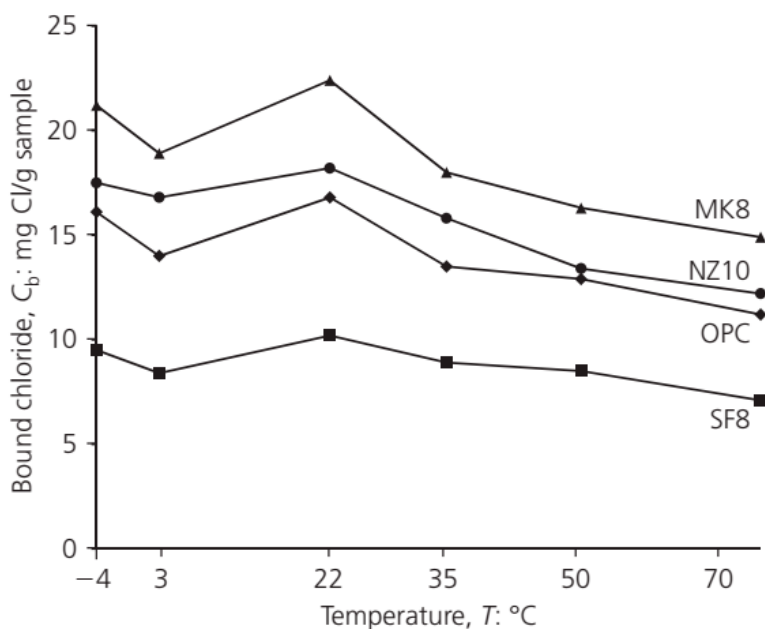


**Figure 13.** Effect of temperature on bound chloride content for different mixtures ( $C_i = 3 \text{ M}$ ). Adapted with permission from Ref. [86].

**Table 3.** Some studies concerning the effect of temperature on chloride binding.

Reference	Range of Temperature	Effect of Increasing Temperature
Wowra and Setzer [119]	0–40 °C	Increase in bound chloride content (due to faster reaction rates at higher temperature)
Hussain and Rasheeduzzafar [120]	20–70 °C	Increased free chloride
CK Larsen 1998 [121] and CK Larsen [122]	20–80 °C	Increase of the chloride concentration of the pore solution
TS Nguyen et al. [123]	5–35 °C (Cl concentration: 0–20 g/L)	No effect

### 5.9. Time and Electrical Field of Accelerated Tests

Accelerated testing for chloride ingress relies on high-voltage electrical fields that increase the rate of transportation of ions through the porous structure of cementitious materials. While different than MK-OPC materials, recent research has demonstrated that the utilization of ND 492 tests (15–30 V), which rely on variable and lower voltages than ASTM C1202 (60 V), yields accurate results for alkali-activated materials and LC3 [124,125]. These results indicate the critical importance of the electric field voltage for comprehensively understanding the transportation of chlorides ions which can be affected by binding phases.

Recent research on MK-OPC materials has demonstrated that chloride binding in these materials is a time-dependent mechanism that does not occur at the early stages of exposure, but rather at yearly scales. Hence, accelerated tests relying on applied voltage to accelerate the rate of transport of chlorides through the material are dissimilar from the natural chloride ingress mechanism. In most cases, such as in the use of ASTM C1202, the effect of the applied electrical field (60 V) on chloride binding is neglected, and there is a critical scientific need to produce a reliable understanding of the electrical field voltage's effect on the chloride transport. Further comprehensive understanding that can account for phases and pore solution chemistries may yield improved accelerated testing of chloride transport. Castellote et al. [126] found that the chloride-binding capacity in accelerated tests is less by 0.14% than the natural experiment in the non-steady-state migration test. These results point to the importance of high electrical fields (high voltage) on the measured chlorides bound from these tests. Ollivier et al. [127] found no difference in the binding capacity in migration tests under 2–30 V—much lower voltages than those specified by ASTM C1202. Furthermore, because of the short duration of accelerated tests, chloride binding is reduced [77]. Consequently, many researchers have relied on non-accelerated tests for chloride ingress that can take into account chloride binding, such as R.M. Ferreira et al. [39]. Therefore, although accelerated tests have certain advantages for evaluating the chloride permeability of concrete and mortar specimens, the potential effect of the applied electrical field on chloride binding is an important and active field of study.

## 6. Conclusions

One of the critical parameters influencing the chloride-induced corrosion requiring further study are chloride-binding mechanisms. Chloride binding is influenced by several factors, one of which is using different SCMs in concrete. One of the SCMs that generally improves chloride binding is MK, mainly due to its high Al content. Considering the recent publication regarding the effect of the MK consumption on the chloride-binding capacity of concrete and other influencing parameters on it, the following conclusion can be made:

1. Chloride binding in specimens containing MK is mostly attributed to chemical chloride binding and Friedel's salt formation, and the proportion of physical chloride binding is usually lower.
2. MK has both negative and positive effects on physical chloride binding. Using MK reduces physical chloride binding by reducing the Ca/Si ratio of CSH, increasing the chain length of CSH, and decreasing the specific surface area of CSH. However, MK increases the physical chloride-binding capacity by increasing the Al/Si ratio of CSH.
3. In the case of the chemical composition of concrete, some studies support the notion that using MK reduces the ettringite and calcite and increases the strätlingite and monosulfoaluminate. However, monocarboaluminate content remains unchanged or increases a bit.
4. In specimens containing MK, monosulfoaluminate (AFm) contributes majorly to Friedel's salt and ettringite formation with NaCl exposure. However, monocarboaluminate makes limited contribution to Friedel's salt formation and chloride binding, and its contribution depends on calcium availability. Therefore, the calcium consumption by the pozzolanic reaction of the MK may reduce the contribution of monocarboaluminate to chloride binding. Strätlingite may also contribute to chloride

binding in high chloride concentrations. However, ettringite does not seem to make a significant and direct contribution to chloride binding.

5. Binding isotherms show the relation between free and binding chlorides. Among binding isotherms, the linear and Langmuir isotherms have acceptable accuracy in low chloride concentrations. However, the BET isotherm is not very popular due to its complexity. Freundlich usually provides the greatest accuracy, especially in conventional sea chloride concentration.
6. Using MK also affects other influential parameters for chloride binding, such as hydro-talcite content and carbonation. Furthermore, some other parameters are influential on chloride binding in the presence of MK, such as sulfate ions, pH, temperature, and electrical fields.
7. MK usually increases carbonation depth, which negatively affects chloride binding. Other parameters that negatively affect chloride binding are increasing temperature, sulfate ions, applied electrical fields, and increasing pH.
8. By augmenting chloride concentration, chloride binding also increases; however, it may reach a plateau and does not increase linearly. Furthermore, in exposure to  $\text{CaCl}_2$  and  $\text{MgCl}_2$ , chloride binding increases, which may be due to improving adsorption mechanism and increasing positive charge of the surface of CSH.

**Author Contributions:** Conceptualization, A.A.R. and R.H.; methodology, R.H.; investigation, R.H.; data curation, R.H.; writing—original draft preparation, R.H., F.M. and A.M.R.; writing—review and editing, R.H., F.M., A.M.R. and J.P.G.; supervision, A.A.R. and F.M.; project administration, A.A.R. All authors have read and agreed to the published version of the manuscript.

**Funding:** This research received no external funding.

**Institutional Review Board Statement:** Not applicable.

**Informed Consent Statement:** Not applicable.

**Data Availability Statement:** Data can be accessed by contacting the following email address: rhomayoonmehr@aut.ac.ir.

**Conflicts of Interest:** The authors declare no conflict of interest.

## References

1. Hanein, T.; Thienel, K.-C.; Zunino, F.; Marsh, A.; Maier, M.; Wang, B.; Canut, M.; Juenger, M.C.; Ben Haha, M.; Avet, F. Clay calcination technology: State-of-the-art review by the RILEM TC 282-CCL. *Mater. Struct.* **2022**, *55*, 3. [[CrossRef](#)]
2. Wang, Y.; Munger, J.; Xu, S.; McElroy, M.B.; Hao, J.; Nielsen, C.; Ma, H.  $\text{CO}_2$  and its correlation with CO at a rural site near Beijing: Implications for combustion efficiency in China. *Atmos. Chem. Phys.* **2010**, *10*, 8881–8897. [[CrossRef](#)]
3. Salas, D.A.; Ramirez, A.D.; Rodríguez, C.R.; Petroche, D.M.; Boero, A.J.; Duque-Rivera, J. Environmental impacts, life cycle assessment and potential improvement measures for cement production: A literature review. *J. Clean. Prod.* **2016**, *113*, 114–122. [[CrossRef](#)]
4. Homayoonmehr, R.; Ramezanianpour, A.A.; Mirdarsoltany, M. Influence of metakaolin on fresh properties, mechanical properties and corrosion resistance of concrete and its sustainability issues: A review. *J. Build. Eng.* **2021**, *44*, 103011. [[CrossRef](#)]
5. Qureshi, L.A.; Ali, B.; Ali, A. Combined effects of supplementary cementitious materials (silica fume, GGBS, fly ash and rice husk ash) and steel fiber on the hardened properties of recycled aggregate concrete. *Constr. Build. Mater.* **2020**, *263*, 120636. [[CrossRef](#)]
6. Masood, B.; Elahi, A.; Barbhuiya, S.; Ali, B. Mechanical and durability performance of recycled aggregate concrete incorporating low calcium bentonite. *Constr. Build. Mater.* **2020**, *237*, 117760. [[CrossRef](#)]
7. Alyousef, R.; Ali, B.; Mohammed, A.; Kurda, R.; Alabduljabbar, H.; Riaz, S. Evaluation of Mechanical and Permeability Characteristics of Microfiber-Reinforced Recycled Aggregate Concrete with Different Potential Waste Mineral Admixtures. *Materials* **2021**, *14*, 5933. [[CrossRef](#)]
8. Barbhuiya, S.; Chow, P.; Memon, S. Microstructure, hydration and nanomechanical properties of concrete containing metakaolin. *Constr. Build. Mater.* **2015**, *95*, 696–702. [[CrossRef](#)]
9. Poon, C.-S.; Lam, L.; Kou, S.; Wong, Y.-L.; Wong, R. Rate of pozzolanic reaction of metakaolin in high-performance cement pastes. *Cem. Concr. Res.* **2001**, *31*, 1301–1306. [[CrossRef](#)]
10. Siddique, R.; Klaus, J. Influence of metakaolin on the properties of mortar and concrete: A review. *Appl. Clay Sci.* **2009**, *43*, 392–400. [[CrossRef](#)]

11. Osio-Norgaard, J.; Gevauan, J.P.; Srubar, W.V., III. A review of chloride transport in alkali-activated cement paste, mortar, and concrete. *Constr. Build. Mater.* **2018**, *186*, 191–206. [[CrossRef](#)]
12. IEA. Cement; IEA: Paris, France, 2020. Available online: <https://www.iea.org/reports/cement> (accessed on 13 November 2022).
13. Peters, G.; Andrew, R.; Canadell, J.; Friedlingstein, P.; Jackson, R.; Korsbakken, J.; Le Quéré, C.; Peregon, A. Carbon dioxide emissions continue to grow amidst slowly emerging climate policies. *Nat. Clim. Change* **2020**, *10*, 3–6. [[CrossRef](#)]
14. Fernandez Pales, A.; Leung, Y. *Technology Roadmap-Low-Carbon Transition in the Cement Industry*; International Energy Agency: Paris, France, 2018. Available online: <https://webstore.iea.org/technologyroadmap-low-carbon-transition-in-the-cement-industry> (accessed on 8 November 2022).
15. Wei, J.; Cen, K. Empirical assessing cement CO<sub>2</sub> emissions based on China’s economic and social development during 2001–2030. *Sci. Total Environ.* **2019**, *653*, 200–211. [[CrossRef](#)] [[PubMed](#)]
16. Sabir, B.; Wild, S.; Bai, J. Metakaolin and calcined clays as pozzolans for concrete: A review. *Cem. Concr. Compos.* **2001**, *23*, 441–454. [[CrossRef](#)]
17. Koch, G.H.; Brongers, M.P.; Thompson, N.G.; Virmani, Y.P.; Payer, J.H. *Corrosion Cost and Preventive Strategies in the United States*; No. FHWA-RD-01-156, R315-01; Federal Highway Administration: Washington, DC, USA, 2002.
18. Di Filippo, J.; Karpman, J.; De Shazo, J. The impacts of policies to reduce CO<sub>2</sub> emissions within the concrete supply chain. *Cem. Concr. Compos.* **2019**, *101*, 67–82. [[CrossRef](#)]
19. Mirdarsoltany, M.; Rahai, A.; Hatami, F.; Homayoonmehr, R.; Abed, F. Investigating Tensile Behavior of Sustainable Basalt–Carbon, Basalt–Steel, and Basalt–Steel-Wire Hybrid Composite Bars. *Sustainability* **2021**, *13*, 10735. [[CrossRef](#)]
20. Mirdarsoltany, M.; Abed, F.; Homayoonmehr, R.; Abad, S.V.A.N.K. A Comprehensive Review of the Effects of Different Simulated Environmental Conditions and Hybridization Processes on the Mechanical Behavior of Different FRP Bars. *Sustainability* **2022**, *14*, 8834. [[CrossRef](#)]
21. Homayoonmehr, R.; Rahai, A.; Ramezanianpour, A.A. Predicting the chloride diffusion coefficient and surface electrical resistivity of concrete using statistical regression-based models and its application in chloride-induced corrosion service life prediction of RC structures. *Constr. Build. Mater.* **2022**, *357*, 129351. [[CrossRef](#)]
22. Gruber, K.; Ramlochan, T.; Boddy, A.; Hooton, R.; Thomas, M. Increasing concrete durability with high-reactivity metakaolin. *Cem. Concr. Compos.* **2001**, *23*, 479–484. [[CrossRef](#)]
23. Li, C.; Xiao, K. Chloride threshold, modelling of corrosion rate and pore structure of concrete with metakaolin addition. *Constr. Build. Mater.* **2021**, *305*, 124666. [[CrossRef](#)]
24. DorMohammadi, H.; Pang, Q.; Murkute, P.; Árnadóttir, L.; Isgor, O.B. Investigation of iron passivity in highly alkaline media using reactive-force field molecular dynamics. *Corros. Sci.* **2019**, *157*, 31–40. [[CrossRef](#)]
25. Furcas, F.E.; Lothenbach, B.; Isgor, O.B.; Mundra, S.; Zhang, Z.; Angst, U.M. Solubility and speciation of iron in cementitious systems. *Cem. Concr. Res.* **2022**, *151*, 106620. [[CrossRef](#)]
26. Käthler, C.B.; Aguilar, A.M.; Angst, U.; Elsener, B. A systematic data collection on chloride-induced steel corrosion in concrete to improve service life modelling and towards understanding corrosion initiation. *Corros. Sci.* **2019**, *157*, 331–336. [[CrossRef](#)]
27. Cao, Y.; Gehlen, C.; Angst, U.; Wang, L.; Wang, Z.; Yao, Y. Critical chloride content in reinforced concrete—An updated review considering Chinese experience. *Cem. Concr. Res.* **2019**, *117*, 58–68. [[CrossRef](#)]
28. Gao, Y.; Zheng, Y.; Zhang, J.; Wang, J.; Zhou, X.; Zhang, Y. Randomness of critical chloride concentration of reinforcement corrosion in reinforced concrete flexural members in a tidal environment. *Ocean. Eng.* **2019**, *172*, 330–341. [[CrossRef](#)]
29. Angst, U.M.; Geiker, M.R.; Alonso, M.C.; Polder, R.; Isgor, O.B.; Elsener, B.; Wong, H.; Michel, A.; Hornbostel, K.; Gehlen, C. The effect of the steel–concrete interface on chloride-induced corrosion initiation in concrete: A critical review by RILEM TC 262-SCI. *Mater. Struct.* **2019**, *52*, 88. [[CrossRef](#)]
30. Yang, L.; Xu, J.; Huang, Y.; Li, L.; Zhao, P.; Lu, L.; Cheng, X.; Zhang, D.; He, Y. Using layered double hydroxides and anion exchange resin to improve the mechanical properties and chloride binding capacity of cement mortars. *Constr. Build. Mater.* **2021**, *272*, 122002. [[CrossRef](#)]
31. Guo, Y.; Zhang, T.; Tian, W.; Wei, J.; Yu, Q. Physically and chemically bound chlorides in hydrated cement pastes: A comparison study of the effects of silica fume and metakaolin. *J. Mater. Sci.* **2019**, *54*, 2152–2169. [[CrossRef](#)]
32. Maes, M.; Gruyaert, E.; De Belie, N. Resistance of concrete with blast-furnace slag against chlorides, investigated by comparing chloride profiles after migration and diffusion. *Mater. Struct.* **2013**, *46*, 89–103. [[CrossRef](#)]
33. Plusquellec, G.; Nonat, A. Interactions between calcium silicate hydrate (CSH) and calcium chloride, bromide and nitrate. *Cem. Concr. Res.* **2016**, *90*, 89–96. [[CrossRef](#)]
34. Zhou, Y.; Hou, D.; Jiang, J.; Liu, L.; She, W.; Yu, J. Experimental and molecular dynamics studies on the transport and adsorption of chloride ions in the nano-pores of calcium silicate phase: The influence of calcium to silicate ratios. *Microporous Mesoporous Mater.* **2018**, *255*, 23–35. [[CrossRef](#)]
35. Zhou, Y.; Hou, D.; Jiang, J.; Wang, P. Chloride ions transport and adsorption in the nano-pores of silicate calcium hydrate: Experimental and molecular dynamics studies. *Constr. Build. Mater.* **2016**, *126*, 991–1001. [[CrossRef](#)]
36. Liu, T.; Yu, Q.; Brouwers, H. In-situ formation of layered double hydroxides (LDHs) in sodium aluminate activated slag: The role of Al-O tetrahedra. *Cem. Concr. Res.* **2022**, *153*, 106697. [[CrossRef](#)]
37. Badogiannis, E.; Aggelis, E.; Papadakis, V.; Tsivilis, S. Evaluation of chloride-penetration resistance of metakaolin concrete by means of a diffusion–Binding model and of the k-value concept. *Cem. Concr. Compos.* **2015**, *63*, 1–7. [[CrossRef](#)]

38. Wang, Y.; Shui, Z.; Gao, X.; Yu, R.; Huang, Y.; Cheng, S. Understanding the chloride binding and diffusion behaviors of marine concrete based on Portland limestone cement-alumina enriched pozzolans. *Constr. Build. Mater.* **2019**, *198*, 207–217. [[CrossRef](#)]
39. Ferreira, R.; Castro-Gomes, J.; Costa, P.; Malheiro, R. Effect of metakaolin on the chloride ingress properties of concrete. *KSCE J. Civ. Eng.* **2016**, *20*, 1375–1384. [[CrossRef](#)]
40. Ramachandran, V.S. Possible states of chloride in the hydration of tricalcium silicate in the presence of calcium chloride. *Matériaux Et Constr.* **1971**, *4*, 3–12. [[CrossRef](#)]
41. Dousti, A.; Beaudoin, J.J.; Shekarchi, M. Chloride binding in hydrated MK, SF and natural zeolite-lime mixtures. *Constr. Build. Mater.* **2017**, *154*, 1035–1047. [[CrossRef](#)]
42. Teymour, M.; Shakouri, M.; Vaddey, N.P. pH-dependent chloride desorption isotherms of Portland cement paste. *Constr. Build. Mater.* **2021**, *312*, 125415. [[CrossRef](#)]
43. Jain, A.; Gencturk, B.; Pirbazari, M.; Dawood, M.; Belarbi, A.; Sohail, M.; Kahraman, R. Influence of pH on chloride binding isotherms for cement paste and its components. *Cem. Concr. Res.* **2021**, *143*, 106378. [[CrossRef](#)]
44. Yuan, Q.; Shi, C.; De Schutter, G.; Audenaert, K.; Deng, D. Chloride binding of cement-based materials subjected to external chloride environment—A review. *Constr. Build. Mater.* **2009**, *23*, 1–13. [[CrossRef](#)]
45. Garcia, R.; de la Rubia, M.; Enriquez, E.; del Campo, A.; Fernandez, J.; Moragues, A. Chloride binding capacity of metakaolin and nanosilica supplementary pozzolanic cementitious materials in aqueous phase. *Constr. Build. Mater.* **2021**, *298*, 123903. [[CrossRef](#)]
46. Florea, M.; Brouwers, H. Chloride binding related to hydration products: Part I: Ordinary Portland Cement. *Cem. Concr. Res.* **2012**, *42*, 282–290. [[CrossRef](#)]
47. Elakneswaran, Y.; Nawa, T.; Kurumisawa, K. Electrokinetic potential of hydrated cement in relation to adsorption of chlorides. *Cem. Concr. Res.* **2009**, *39*, 340–344. [[CrossRef](#)]
48. Alizadeh, R.A. *Nanostructure and Engineering Properties of Basic and Modified Calcium-Silicate-Hydrate Systems*; University of Ottawa: Ottawa, ON, Canada, 2009; Volume 71.
49. Beaudoin, J.J.; Ramachandran, V.S.; Feldman, R.F. Interaction of chloride and C–S–H. *Cem. Concr. Res.* **1990**, *20*, 875–883. [[CrossRef](#)]
50. Shi, Z.; Geiker, M.R.; De Weerdt, K.; Østnor, T.A.; Lothenbach, B.; Winnefeld, F.; Skibsted, J. Role of calcium on chloride binding in hydrated Portland cement–metakaolin–limestone blends. *Cem. Concr. Res.* **2017**, *95*, 205–216. [[CrossRef](#)]
51. Brykov, A.; Krasnobaeva, S.; Mokeev, M. Hydration of Portland cement in the presence of highly reactive metakaolin. *Mater. Sci. Appl.* **2015**, *6*, 391. [[CrossRef](#)]
52. Qomi, M.A.; Krakowiak, K.; Bauchy, M.; Stewart, K.; Shahsavari, R.; Jagannathan, D.; Brommer, D.B.; Baronnet, A.; Buehler, M.J.; Yip, S. Combinatorial molecular optimization of cement hydrates. *Nat. Commun.* **2014**, *5*, 4960. [[CrossRef](#)]
53. Wilson, W.; Gonthier, J.N.; Georget, F.; Scrivener, K.L. Insights on chemical and physical chloride binding in blended cement pastes. *Cem. Concr. Res.* **2022**, *156*, 106747. [[CrossRef](#)]
54. Zhao, D.; Khoshnazar, R. Microstructure of cement paste incorporating high volume of low-grade metakaolin. *Cem. Concr. Compos.* **2020**, *106*, 103453. [[CrossRef](#)]
55. Avet, F.; Scrivener, K. Investigation of the calcined kaolinite content on the hydration of Limestone Calcined Clay Cement (LC3). *Cem. Concr. Res.* **2018**, *107*, 124–135. [[CrossRef](#)]
56. Maraghechi, H.; Avet, F.; Wong, H.; Kamyab, H.; Scrivener, K. Performance of Limestone Calcined Clay Cement (LC3) with various kaolinite contents with respect to chloride transport. *Mater. Struct.* **2018**, *51*, 125. [[CrossRef](#)]
57. Babaahmadi, A.; Machner, A.; Kunther, W.; Figueira, J.; Hemstad, P.; De Weerdt, K. Chloride binding in Portland composite cements containing metakaolin and silica fume. *Cem. Concr. Res.* **2022**, *161*, 106924. [[CrossRef](#)]
58. Dai, Z.; Tran, T.T.; Skibsted, J. Aluminum Incorporation in the C–S–H phase of white Portland cement–metakaolin blends studied by 27 Al and 29 Si MAS NMR spectroscopy. *J. Am. Ceram. Soc.* **2014**, *97*, 2662–2671. [[CrossRef](#)]
59. Love, C.; Richardson, I.; Brough, A. Composition and structure of C–S–H in white Portland cement–20% metakaolin pastes hydrated at 25 °C. *Cem. Concr. Res.* **2007**, *37*, 109–117. [[CrossRef](#)]
60. Elakneswaran, Y.; Iwasa, A.; Nawa, T.; Sato, T.; Kurumisawa, K. Ion–cement hydrate interactions govern multi-ionic transport model for cementitious materials. *Cem. Concr. Res.* **2010**, *40*, 1756–1765. [[CrossRef](#)]
61. Henocq, P.; Marchand, J.; Samson, E.; Lavoie, J.-A. Modeling of ionic interactions at the C–S–H surface—Application to CsCl and LiCl solutions in comparison with NaCl solutions. In Proceedings of the 2nd International Symposium on Advances in Concrete through Science and Engineering, RILEM Proceedings, Quebec City, QC, Canada, 11–13 September 2006; RILEM Publications: Lyon, France, 2006.
62. Lambert, P.; Page, C.; Short, N. Pore solution chemistry of the hydrated system tricalcium silicate/sodium chloride/water. *Cem. Concr. Res.* **1985**, *15*, 675–680. [[CrossRef](#)]
63. Talero, R.; Trusilewicz, L. Morphological differentiation and crystal growth form of Friedel's salt originated from pozzolan and Portland cement. *Ind. Eng. Chem. Res.* **2012**, *51*, 12517–12529. [[CrossRef](#)]
64. Gbozee, M.; Zheng, K.; He, F.; Zeng, X. The influence of aluminum from metakaolin on chemical binding of chloride ions in hydrated cement pastes. *Appl. Clay Sci.* **2018**, *158*, 186–194. [[CrossRef](#)]
65. Baquerizo, L.G.; Matschei, T.; Scrivener, K.L.; Saeidpour, M.; Wadsö, L. Hydration states of AFm cement phases. *Cem. Concr. Res.* **2015**, *73*, 143–157. [[CrossRef](#)]
66. Justnes, H. A review of chloride binding in cementitious systems. *Nord. Concr. Res. Publ.* **1998**, *21*, 48–63.

67. Suryavanshi, A.; Scantlebury, J.; Lyon, S. Mechanism of Friedel's salt formation in cements rich in tri-calcium aluminate. *Cem. Concr. Res.* **1996**, *26*, 717–727. [\[CrossRef\]](#)
68. Wang, Y.; Shui, Z.; Gao, X.; Huang, Y.; Yu, R.; Ling, G. Chloride binding behaviors of metakaolin-lime hydrated blends: Influence of gypsum and atmospheric carbonation. *Constr. Build. Mater.* **2019**, *201*, 380–390. [\[CrossRef\]](#)
69. De Weerdt, K.; Colombo, A.; Coppola, L.; Justnes, H.; Geiker, M.R. Impact of the associated cation on chloride binding of Portland cement paste. *Cem. Concr. Res.* **2015**, *68*, 196–202. [\[CrossRef\]](#)
70. Antoni, M.; Rossen, J.; Martirena, F.; Scrivener, K. Cement substitution by a combination of metakaolin and limestone. *Cem. Concr. Res.* **2012**, *42*, 1579–1589. [\[CrossRef\]](#)
71. Zibara, H.; Hooton, R.; Thomas, M.; Stanish, K. Influence of the C/S and C/A ratios of hydration products on the chloride ion binding capacity of lime-SF and lime-MK mixtures. *Cem. Concr. Res.* **2008**, *38*, 422–426. [\[CrossRef\]](#)
72. Chen, J.; Ng, P.; Chu, S.; Guan, G.; Kwan, A. Ternary blending with metakaolin and silica fume to improve packing density and performance of binder paste. *Constr. Build. Mater.* **2020**, *252*, 119031. [\[CrossRef\]](#)
73. Ekolu, S.; Thomas, M.; Hooton, R. Pessimum effect of externally applied chlorides on expansion due to delayed ettringite formation: Proposed mechanism. *Cem. Concr. Res.* **2006**, *36*, 688–696. [\[CrossRef\]](#)
74. Wang, Y.; Shui, Z.; Huang, Y.; Sun, T.; Duan, P. Properties of coral waste-based mortar incorporating metakaolin: Part II. Chloride migration and binding behaviors. *Constr. Build. Mater.* **2018**, *174*, 433–442. [\[CrossRef\]](#)
75. Balonis, M.; Lothenbach, B.; Saout, G.L.; Glasser, F.P. Impact of chloride on the mineralogy of hydrated Portland cement systems. *Cem. Concr. Res.* **2010**, *40*, 1009–1022. [\[CrossRef\]](#)
76. Matschei, T.; Lothenbach, B.; Glasser, F. The AFm phase in Portland cement. *Cem. Concr. Res.* **2007**, *37*, 118–130. [\[CrossRef\]](#)
77. Wang, Y.; Shui, Z.; Yu, R.; Huang, Y. Chloride ingress and binding of coral waste filler-coral waste sand marine mortar incorporating metakaolin. *Constr. Build. Mater.* **2018**, *190*, 1069–1080. [\[CrossRef\]](#)
78. Shi, Z.; Geiker, M.R.; Lothenbach, B.; De Weerdt, K.; Garzón, S.F.; Enemark-Rasmussen, K.; Skibsted, J. Friedel's salt profiles from thermogravimetric analysis and thermodynamic modelling of Portland cement-based mortars exposed to sodium chloride solution. *Cem. Concr. Compos.* **2017**, *78*, 73–83. [\[CrossRef\]](#)
79. Hirao, H.; Yamada, K.; Takahashi, H.; Zibara, H. Chloride binding of cement estimated by binding isotherms of hydrates. *J. Adv. Concr. Technol.* **2005**, *3*, 77–84. [\[CrossRef\]](#)
80. Thomas, M.; Hooton, R.; Scott, A.; Zibara, H. The effect of supplementary cementitious materials on chloride binding in hardened cement paste. *Cem. Concr. Res.* **2012**, *42*, 1–7. [\[CrossRef\]](#)
81. Luping, T.; Nilsson, L.-O. Chloride binding capacity and binding isotherms of OPC pastes and mortars. *Cem. Concr. Res.* **1993**, *23*, 247–253. [\[CrossRef\]](#)
82. Yi, C.; Ma, H.; Zhu, H.; Li, W.; Xin, M.; Liu, Y.; Guo, Y. Study on chloride binding capability of coal gangue based cementitious materials. *Constr. Build. Mater.* **2018**, *167*, 649–656. [\[CrossRef\]](#)
83. Ipavec, A.; Vuk, T.; Gabrovšek, R.; Kaučič, V. Chloride binding into hydrated blended cements: The influence of limestone and alkalinity. *Cem. Concr. Res.* **2013**, *48*, 74–85. [\[CrossRef\]](#)
84. Fu, C.; Jin, X.; Jin, N. Modeling of Chloride Ions Diffusion in Cracked Concrete. In *Earth and Space 2010*; American Society of Civil Engineers: Reston, VA, USA, 2010; pp. 3579–3589.
85. Martin-Pérez, B.; Zibara, H.; Hooton, R.; Thomas, M. A study of the effect of chloride binding on service life predictions. *Cem. Concr. Res.* **2000**, *30*, 1215–1223. [\[CrossRef\]](#)
86. Dousti, A.; Shekarchi, M. Effect of exposure temperature on chloride-binding capacity of cementing materials. *Mag. Concr. Res.* **2015**, *67*, 821–832. [\[CrossRef\]](#)
87. Kayali, O.; Khan, M.; Ahmed, M.S. The role of hydrotalcite in chloride binding and corrosion protection in concretes with ground granulated blast furnace slag. *Cem. Concr. Compos.* **2012**, *34*, 936–945. [\[CrossRef\]](#)
88. Ye, H.; Jin, X.; Chen, W.; Fu, C.; Jin, N. Prediction of chloride binding isotherms for blended cements. *Comput. Concr.* **2016**, *17*, 655–672. [\[CrossRef\]](#)
89. Machner, A.; Zajac, M.; Haha, M.B.; Kjellsen, K.O.; Geiker, M.R.; De Weerdt, K. Chloride-binding capacity of hydrotalcite in cement pastes containing dolomite and metakaolin. *Cem. Concr. Res.* **2018**, *107*, 163–181. [\[CrossRef\]](#)
90. Machner, A.; Zajac, M.; Haha, M.B.; Kjellsen, K.O.; Geiker, M.R.; De Weerdt, K. Limitations of the hydrotalcite formation in Portland composite cement pastes containing dolomite and metakaolin. *Cem. Concr. Res.* **2018**, *105*, 1–17. [\[CrossRef\]](#)
91. Taylor, R.; Richardson, I.; Brydson, R. Composition and microstructure of 20-year-old ordinary Portland cement-ground granulated blast-furnace slag blends containing 0 to 100% slag. *Cem. Concr. Res.* **2010**, *40*, 971–983. [\[CrossRef\]](#)
92. Haha, M.B.; Lothenbach, B.; Le Saout, G.; Winnefeld, F. Influence of slag chemistry on the hydration of alkali-activated blast-furnace slag—Part II: Effect of  $\text{Al}_2\text{O}_3$ . *Cem. Concr. Res.* **2012**, *42*, 74–83. [\[CrossRef\]](#)
93. Miyata, S. The Syntheses of Hydrotalcite-Like Compounds and Their Structures and Physico-Chemical Properties—I: The Systems  $\text{Mg}^{2+}\text{-Al}^{3+}\text{-NO}_3^-$ ,  $\text{Mg}^{2+}\text{-Al}^{3+}\text{-Cl}^-$ ,  $\text{Mg}^{2+}\text{-Al}^{3+}\text{-ClO}_4^-$ ,  $\text{Ni}^{2+}\text{-Al}^{3+}\text{-Cl}^-$  and  $\text{Zn}^{2+}\text{-Al}^{3+}\text{-Cl}^-$ . *Clays Clay Miner.* **1975**, *23*, 369–375. [\[CrossRef\]](#)
94. Žemlička, M.; Kuzielova, E.; Kuliffayova, M.; Tkacz, J.; Palou, M.T. Study of hydration products in the model systems metakaolin-lime and metakaolin-lime-gypsum. *Ceram. Silik.* **2015**, *59*, 283–291.
95. Cheewaket, T.; Jaturapitakkul, C.; Chalee, W. Long term performance of chloride binding capacity in fly ash concrete in a marine environment. *Constr. Build. Mater.* **2010**, *24*, 1352–1357. [\[CrossRef\]](#)

96. Wang, G.; Kong, Y.; Shui, Z.; Li, Q.; Han, J. Experimental investigation on chloride diffusion and binding in concrete containing metakaolin. *Corros. Eng. Sci. Technol.* **2014**, *49*, 282–286. [[CrossRef](#)]
97. Babu, U.R.; Kondraivendhan, B. Application of Statistics to the Analysis of Corrosion Data for Rebar in Metakaolin Concrete. In Proceedings of the International Conference on Emerging Trends in Engineering (ICETE), Hyderabad, India, 22–23 March 2019; Springer: Berlin/Heidelberg, Germany, 2020; pp. 162–169.
98. Yang, L.; Yu, H.; Ma, H.; Zhou, P. Deterioration of high performance hybrid fibers reinforced expansive concrete exposed to magnesium sulfate solution. In Proceedings of the International Conference on Transportation Engineering 2009, Chengdu, China, 25–27 July 2009; pp. 2614–2619.
99. Olivier, T. Prediction of Chloride Penetration into Saturated Concrete-Multi-Species Approach. Ph.D. Thesis, Department of Building Materials Chalmers University of Technology, Gothenburg, Sweden, 2000.
100. Saillio, M.; Baroghel-Bouny, V.; Barberon, F. Chloride binding in sound and carbonated cementitious materials with various types of binder. *Constr. Build. Mater.* **2014**, *68*, 82–91. [[CrossRef](#)]
101. Ma, J.; Li, Z. Chemical Equilibrium Modeling and Experimental Measurement of Solubility for Friedel’s Salt in the Na–OH–Cl–NO<sub>3</sub>–H<sub>2</sub>O Systems up to 200 °C. *Ind. Eng. Chem. Res.* **2010**, *49*, 8949–8958. [[CrossRef](#)]
102. Page, C.; Vennesland, Ø. Pore solution composition and chloride binding capacity of silica-fume cement pastes. *Matériaux Constr.* **1983**, *16*, 19–25. [[CrossRef](#)]
103. Labbez, C.; Pochard, I.; Jönsson, B.; Nonat, A. CSH/solution interface: Experimental and Monte Carlo studies. *Cem. Concr. Res.* **2011**, *41*, 161–168. [[CrossRef](#)]
104. Liu, W.; Cui, H.; Dong, Z.; Xing, F.; Zhang, H.; Lo, T.Y. Carbonation of concrete made with dredged marine sand and its effect on chloride binding. *Constr. Build. Mater.* **2016**, *120*, 1–9. [[CrossRef](#)]
105. Damidot, D.; Atkins, M.; Kindness, A.; Glasser, F. Sulphate attack on concrete: Limits of the AFt stability domain. *Cem. Concr. Res.* **1992**, *22*, 229–234. [[CrossRef](#)]
106. Gabrisova, A.; Havlica, J.; Sahu, S. Stability of calcium sulphaaluminate hydrates in water solutions with various pH values. *Cem. Concr. Res.* **1991**, *21*, 1023–1027. [[CrossRef](#)]
107. Glass, G.; Buenfeld, N. The influence of chloride binding on the chloride induced corrosion risk in reinforced concrete. *Corros. Sci.* **2000**, *42*, 329–344. [[CrossRef](#)]
108. Zhu, Q.; Jiang, L.; Chen, Y.; Xu, J.; Mo, L. Effect of chloride salt type on chloride binding behavior of concrete. *Constr. Build. Mater.* **2012**, *37*, 512–517. [[CrossRef](#)]
109. De Weerdt, K.; Orsáková, D.; Geiker, M.R. The impact of sulphate and magnesium on chloride binding in Portland cement paste. *Cem. Concr. Res.* **2014**, *65*, 30–40. [[CrossRef](#)]
110. Lothenbach, B.; Scrivener, K.; Hooton, R. Supplementary cementitious materials. *Cem. Concr. Res.* **2011**, *41*, 1244–1256. [[CrossRef](#)]
111. AASHTO. *Designation: T 358-15—Standard Method of Test for Surface Resistivity Indication of Concrete’s Ability to Resist Chloride Ion Penetration*; American Association of State Highway and Transportation Officials: Washington, DC, USA, 2015.
112. Shahidan, S.; Tayeh, B.A.; Jamaludin, A.; Bahari, N.; Mohd, S.; Ali, N.Z.; Khalid, F. *Physical and Mechanical Properties of Self-Compacting Concrete Containing Superplasticizer and Metakaolin*; IOP Conference Series: Materials Science and Engineering; IOP Publishing: Bristol, UK, 2017; p. 012004.
113. Hassan, Z. *Binding of External Chloride by Cement Pastes*; University of Toronto: Toronto, ON, Canada, 2001.
114. Plusquellec, G.; Nonat, A.; Pochard, I. Anion uptake by calcium silicate hydrate. In Proceedings of the 32nd Cement and Concrete Science Conference, Belfast, Northern Ireland, 17–18 September 2012; pp. 17–18.
115. Vieira, D.R.; Moreira, A.L.R.; Calmon, J.L.; Dominicini, W.K. Service life modeling of a bridge in a tropical marine environment for durable design. *Constr. Build. Mater.* **2018**, *163*, 315–325. [[CrossRef](#)]
116. Dousti, A.; Rashetnia, R.; Ahmadi, B.; Shekarchi, M. Influence of exposure temperature on chloride diffusion in concretes incorporating silica fume or natural zeolite. *Constr. Build. Mater.* **2013**, *49*, 393–399. [[CrossRef](#)]
117. Rostam, S. Service Life Design of Concrete Structures—a Challenge to Designers as Well as to Owners. *Asian J. Civ. Eng.* **2005**, *6*, 423–445.
118. Panesar, D.; Chidiac, S. Effect of cold temperature on the chloride-binding capacity of cement. *J. Cold Reg. Eng.* **2011**, *25*, 133–144. [[CrossRef](#)]
119. Wowra, O.; Setzer, M.; Setzer, M.; Auberg, R. Sorption of chlorides on hydrated cements and C3S pastes. In *Frost Resistance of Concrete*; CRC Press: Boca Raton, FL, USA, 1997; pp. 147–153.
120. Hussain, S.E. Effect of temperature on pore solution composition in plain cements. *Cem. Concr. Res.* **1993**, *23*, 1357–1368. [[CrossRef](#)]
121. Larsen, C. Chloride Binding in Concrete—Effect of Surrounding Environment and Concrete Composition. Dr. Ing. Thesis, NTNU, Trondheim, Norway, 1998.
122. Larsen, C.K. *Effect of Type of Aggregate, Temperature and Drying/Rewetting on Chloride Binding and Pore Solution Composition*; RILEM: Bagneux, France, 1997; Volume 27.
123. Nguyen, T.; Lorente, S.; Carcasses, M. Effect of the environment temperature on the chloride diffusion through CEM-I and CEM-V mortars: An experimental study. *Constr. Build. Mater.* **2009**, *23*, 795–803. [[CrossRef](#)]
124. Wilson, W.; Georget, F.; Scrivener, K. Unravelling chloride transport/microstructure relationships for blended-cement pastes with the mini-migration method. *Cem. Concr. Res.* **2021**, *140*, 106264. [[CrossRef](#)]

125. Gluth, G.J.; Arbi, K.; Bernal, S.A.; Bondar, D.; Castel, A.; Chithiraputhiran, S.; Dehghan, A.; Dombrowski-Daube, K.; Dubey, A.; Ducman, V. RILEM TC 247-DTA round robin test: Carbonation and chloride penetration testing of alkali-activated concretes. *Mater. Struct.* **2020**, *53*, 21. [[CrossRef](#)]
126. Castellote, M.; Andrade, C.; Alonso, C. Chloride-binding isotherms in concrete submitted to non-steady-state migration experiments. *Cem. Concr. Res.* **1999**, *29*, 1799–1806. [[CrossRef](#)]
127. Ollivier, J.; Arsenault, J.; Truc, O.; Marchand, J. Determination of chloride binding isotherms from migration tests. In Proceedings of the Mario Collepardi Symposium on Advances in Concrete Science and Technology, Rome, Italy, 7 October 1997; pp. 198–217.